



# Limit on the production of a light vector gauge boson in $\phi$ meson decays with the KLOE detector

KLOE-2 Collaboration

D. Babusci<sup>h</sup>, D. Badoni<sup>r,s</sup>, I. Balwierz-Pytko<sup>g</sup>, G. Bencivenni<sup>h</sup>, C. Bini<sup>p,q</sup>, C. Bloise<sup>h</sup>, F. Bossi<sup>h</sup>, P. Branchini<sup>u</sup>, A. Budano<sup>t,u</sup>, L. Caldeira Balkestahl<sup>w</sup>, G. Capon<sup>h</sup>, F. Ceradini<sup>t,u</sup>, P. Ciambrone<sup>h</sup>, E. Czerwiński<sup>g</sup>, E. Danè<sup>h</sup>, E. De Lucia<sup>h</sup>, G. De Robertis<sup>b</sup>, A. De Santis<sup>p,q</sup>, A. Di Domenico<sup>p,q</sup>, C. Di Donato<sup>l,m</sup>, R. Di Salvo<sup>s</sup>, D. Domenici<sup>h</sup>, O. Erriquez<sup>a,b</sup>, G. Fanizzi<sup>a,b</sup>, A. Fantini<sup>r,s</sup>, G. Felici<sup>h</sup>, S. Fiore<sup>p,q</sup>, P. Franzini<sup>p,q</sup>, P. Gauzzi<sup>p,q</sup>, G. Giardina<sup>j,d</sup>, S. Giovannella<sup>h,\*</sup>, F. Gonnella<sup>r,s</sup>, E. Graziani<sup>u</sup>, F. Happacher<sup>h</sup>, L. Heijenskjöld<sup>w</sup>, B. Höistad<sup>w</sup>, L. Iafolla<sup>h</sup>, M. Jacewicz<sup>w</sup>, T. Johansson<sup>w</sup>, A. Kupsc<sup>w</sup>, J. Lee-Franzini<sup>h,v</sup>, B. Leverington<sup>h</sup>, F. Loddo<sup>b</sup>, S. Loffredo<sup>t,u</sup>, G. Mandaglio<sup>j,d,c</sup>, M. Martemianov<sup>k</sup>, M. Martini<sup>h,o</sup>, M. Mascolo<sup>r,s</sup>, R. Messi<sup>r,s</sup>, S. Miscetti<sup>h</sup>, G. Morello<sup>h</sup>, D. Moricciani<sup>s</sup>, P. Moskal<sup>g</sup>, F. Nguyen<sup>u,1</sup>, A. Passeri<sup>u</sup>, V. Patera<sup>n,h</sup>, I. Prado Longhi<sup>t,u</sup>, A. Ranieri<sup>b</sup>, C.F. Redmer<sup>i</sup>, P. Santangelo<sup>h</sup>, I. Sarra<sup>h,\*</sup>, M. Schioppa<sup>e,f</sup>, B. Sciascia<sup>h</sup>, M. Silarski<sup>g</sup>, C. Taccini<sup>t,u</sup>, L. Tortora<sup>u</sup>, G. Venanzoni<sup>h</sup>, W. Wiślicki<sup>x</sup>, M. Wolke<sup>w</sup>, J. Zdebik<sup>g</sup>

<sup>a</sup> Dipartimento di Fisica dell'Università di Bari, Bari, Italy

<sup>b</sup> INFN Sezione di Bari, Bari, Italy

<sup>c</sup> Centro Siciliano di Fisica Nucleare e Struttura della Materia, Catania, Italy

<sup>d</sup> INFN Sezione di Catania, Catania, Italy

<sup>e</sup> Dipartimento di Fisica dell'Università della Calabria, Cosenza, Italy

<sup>f</sup> INFN Gruppo collegato di Cosenza, Cosenza, Italy

<sup>g</sup> Institute of Physics, Jagiellonian University, Cracow, Poland

<sup>h</sup> Laboratori Nazionali di Frascati dell'INFN, Frascati, Italy

<sup>i</sup> Institut für Kernphysik, Johannes Gutenberg Universität Mainz, Germany

<sup>j</sup> Dipartimento di Fisica e Scienze della Terra dell'Università di Messina, Messina, Italy

<sup>k</sup> Institute for Theoretical and Experimental Physics (ITEP), Moscow, Russia

<sup>l</sup> Dipartimento di Fisica dell'Università "Federico II", Napoli, Italy

<sup>m</sup> INFN Sezione di Napoli, Napoli, Italy

<sup>n</sup> Dipartimento di Scienze di Base ed Applicate per l'Ingegneria dell'Università "Sapienza", Roma, Italy

<sup>o</sup> Dipartimento di Scienze e Tecnologie applicate, Università "Guglielmo Marconi", Roma, Italy

<sup>p</sup> Dipartimento di Fisica dell'Università "Sapienza", Roma, Italy

<sup>q</sup> INFN Sezione di Roma, Roma, Italy

<sup>r</sup> Dipartimento di Fisica dell'Università "Tor Vergata", Roma, Italy

<sup>s</sup> INFN Sezione di Roma Tor Vergata, Roma, Italy

<sup>t</sup> Dipartimento di Fisica dell'Università "Roma Tre", Roma, Italy

<sup>u</sup> INFN Sezione di Roma Tre, Roma, Italy

<sup>v</sup> Physics Department, State University of New York at Stony Brook, NY, USA

<sup>w</sup> Department of Physics and Astronomy, Uppsala University, Uppsala, Sweden

<sup>x</sup> National Centre for Nuclear Research, Warsaw, Poland

## ARTICLE INFO

### Article history:

Received 15 October 2012

Received in revised form 29 January 2013

Accepted 31 January 2013

Available online 6 February 2013

Editor: M. Doser

## ABSTRACT

We present a new limit on the production of a light dark-force mediator with the KLOE detector at DAΦNE. This boson, called  $U$ , has been searched for in the decay  $\phi \rightarrow \eta U$ ,  $U \rightarrow e^+e^-$ , analyzing the decay  $\eta \rightarrow \pi^0\pi^0\pi^0$  in a data sample of  $1.7 \text{ fb}^{-1}$ . No structures are observed in the  $e^+e^-$  invariant mass distribution over the background. This search is combined with a previous result obtained from the decay  $\eta \rightarrow \pi^+\pi^-\pi^0$ , increasing the sensitivity. We set an upper limit at 90% C.L. on the ratio between

\* Corresponding authors.

E-mail addresses: [simona.giovannella@lnf.infn.it](mailto:simona.giovannella@lnf.infn.it) (S. Giovannella), [ivano.sarra@lnf.infn.it](mailto:ivano.sarra@lnf.infn.it) (I. Sarra).

<sup>1</sup> Present address: Laboratório de Instrumentação e Física Experimental de Partículas, Lisbon, Portugal.

**Keywords:**

$e^+e^-$  Collisions  
Dark forces  
Gauge vector boson

the  $U$  boson coupling constant and the fine structure constant of  $\alpha'/\alpha < 1.7 \times 10^{-5}$  for  $30 < M_U < 400$  MeV and  $\alpha'/\alpha \leq 8 \times 10^{-6}$  for the sub-region  $50 < M_U < 210$  MeV. This result assumes the Vector Meson Dominance expectations for the  $\phi\eta\gamma^*$  transition form factor. The dependence of this limit on the transition form factor has also been studied.

© 2013 Elsevier B.V. All rights reserved.

## 1. Introduction

There are theories beyond the Standard Model (SM) that postulate the existence of new bosons, mediators of some hidden gauge group, under which ordinary matter is uncharged [1,2]. Such theories have been recently invoked to account for some puzzling astrophysical observations and predict that at least one of the new bosons is neutral, relatively light and weakly coupled with ordinary matter [3,4]. The coupling is represented by adding to the Lagrangian a kinetic mixing term [5] between the new ( $U$ ) boson and the photon, whose strength is measured by a parameter  $\epsilon$  that could be as large as  $\sim 10^{-3}$ . Due to this mixing, the  $U$  boson can be produced in processes involving SM particles, and can decay into  $e^+e^-$ ,  $\mu^+\mu^-$ ,  $\pi^+\pi^-$ , ..., depending on its mass and on model-specific details.

Searches for the  $U$  boson have been recently performed at  $e$ - $p$  fixed target facilities [6,7], and, in conjunction with a dark Higgs, at  $e^+e^-$  colliders [8], with null results. The  $U$  can also be searched for in vector ( $V$ ) to pseudoscalar ( $P$ ) meson decays, with a rate that is  $\epsilon^2$  times suppressed with respect to the ordinary  $V \rightarrow P\gamma$  transitions [9]. Since the  $U$  is supposed to decay to  $e^+e^-$  with a non-negligible branching ratio,  $V \rightarrow PU$  events will produce a sharp peak in the invariant mass distribution of the electron-positron pair over the continuum background due to Dalitz decay events  $V \rightarrow Pe^+e^-$ . Using this approach, KLOE has already published a limit on the existence of the  $U$  boson [10], studying  $\phi \rightarrow \eta e^+e^-$  decays, where the  $\eta$  meson was tagged by its  $\pi^+\pi^-\pi^0$  decay. In this Letter, we present an update of this analysis, which improves background rejection for the already used data sample ( $1.5 \text{ fb}^{-1}$ ) and increases statistics by a factor of about three, exploiting also the neutral  $\eta \rightarrow \pi^0\pi^0\pi^0$  decay chain, with a data sample of  $1.7 \text{ fb}^{-1}$ .

## 2. The KLOE detector

DAΦNE, the Frascati  $\phi$ -factory, is an  $e^+e^-$  collider running at center-of-mass energy of  $\sim 1020$  MeV. Positron and electron beams collide at an angle of  $\pi-25$  mrad, producing  $\phi$  mesons nearly at rest. The KLOE experiment operated at this collider from 2000 to 2006, collecting  $2.5 \text{ fb}^{-1}$ . The KLOE detector consists of a large cylindrical Drift Chamber (DC), surrounded by a lead-scintillating fiber electromagnetic calorimeter (EMC), all embedded inside a superconducting coil, providing a 0.52 T axial field. The beam pipe at the interaction region is a sphere with 10 cm radius, made of a 0.5 mm thick beryllium–aluminum alloy. The drift chamber [11], 4 m in diameter and 3.3 m long, has 12582 all-stereo tungsten sense wires and 37746 aluminum field wires, with a shell made of carbon fiber-epoxy composite with an internal wall of  $\sim 1$  mm thickness. The gas used is a 90% helium, 10% isobutane mixture. The momentum resolution is  $\sigma(p_\perp)/p_\perp \approx 0.4\%$ . Vertices are reconstructed with a spatial resolution of  $\sim 3$  mm. The calorimeter [12], with a readout granularity of  $\sim (4.4 \times 4.4) \text{ cm}^2$ , for a total of 2440 cells arranged in five layers, covers 98% of the solid angle. Each cell is read out at both ends by photomultipliers, both in amplitude and time. The energy deposits are obtained from the signal amplitude while the arrival times and the particles positions are obtained from the time dif-

ferences. Cells close in time and space are grouped into energy clusters. Energy and time resolutions are  $\sigma_E/E = 5.7\%/\sqrt{E}$  (GeV) and  $\sigma_t = 57 \text{ ps}/\sqrt{E}$  (GeV)  $\oplus 100$  ps, respectively. The trigger [13] uses both calorimeter and chamber information. In this analysis the events are selected by the calorimeter trigger, requiring two energy deposits with  $E > 50$  MeV for the barrel and  $E > 150$  MeV for the endcaps. Data are then analyzed by an event classification filter [14], which selects and streams various categories of events in different output files.

## 3. Event selection

To improve the search for the  $U$  boson, we have carried out the analysis of the process  $\phi \rightarrow \eta U$ ,  $U \rightarrow e^+e^-$ , adding the decay channel  $\eta \rightarrow \pi^0\pi^0\pi^0$  to the previously used,  $\eta \rightarrow \pi^+\pi^-\pi^0$ . The new search has been performed on a data sample of  $1.7 \text{ fb}^{-1}$ , corresponding approximately to  $6 \times 10^9$  produced  $\phi$  mesons. The Monte Carlo (MC) simulation for the  $\phi \rightarrow \eta U$  decay has been developed according to [9], with a flat distribution in the  $e^+e^-$  invariant mass,  $M_{ee}$ , while the irreducible background  $\phi \rightarrow \eta e^+e^-$ ,  $\eta \rightarrow \pi\pi\pi$ , has been simulated according to a Vector Meson Dominance parametrization [15]. All MC productions, including all other  $\phi$  decays, take into account changes in DAΦNE operation and background conditions on a run-by-run basis. Corrections for data-MC discrepancies in cluster energies and tracking efficiency, evaluated with radiative Bhabha scattering and  $\phi \rightarrow \rho\pi$  event samples, respectively, have been applied.

As a first analysis step for the neutral  $\eta$  decay channel, a preselection is performed requiring:

- (1) two opposite charge tracks with point of closest approach to the beam line inside a cylinder around the interaction point (IP), of 4 cm transverse radius and 20 cm length;
- (2) six prompt photon candidates, *i.e.* energy clusters with  $E > 7$  MeV not associated to any track, in an angular acceptance  $|\cos\theta_\gamma| < 0.92$  and in the expected time window for a photon ( $|T_\gamma - R_\gamma/c| < \text{MIN}(3\sigma_t, 2 \text{ ns})$ );
- (3) a loose cut on the six-photon invariant mass:  $400 < M_{6\gamma} < 700$  MeV.

After this selection, a peak corresponding to the  $\eta$  mass is clearly observed in the distribution of the recoil mass against the  $e^+e^-$  pair,  $M_{\text{recoil}}(ee)$  (Fig. 1). The second peak at  $\sim 590$  MeV is due to  $K_S \rightarrow \pi^+\pi^-$  decays with wrong mass assignment. To select  $\phi \rightarrow \eta e^+e^-$  events, a  $3\sigma$  cut is applied on this variable,  $536.5 < M_{\text{recoil}}(ee) < 554.5$  MeV. The retained sample has  $\sim 20\%$  residual background contamination, constituted by  $\phi \rightarrow \eta\gamma$ ,  $\phi \rightarrow K_S K_L$  and  $e^+e^- \rightarrow \omega\pi^0$  (about 50%, 35% and 15% of the whole background contribution, respectively). In Fig. 2, the comparison between data and Monte Carlo events for the  $M_{ee}$  and  $\cos\Psi^*$  distributions is shown at this analysis level. The  $\Psi^*$  variable is the angle between the directions of the  $\eta$  and the  $e^+$  in the  $e^+e^-$  rest frame. Photon conversion events are concentrated at  $M_{ee} \sim 30$  MeV and  $\cos\Psi^* < 0.6$ , while the other backgrounds cover the  $M_{ee} > 300$  MeV region and are uniformly distributed in  $\cos\Psi^*$ .

The  $\phi \rightarrow \eta\gamma$  background contamination is mainly due to events where a photon converts to an  $e^+e^-$  pair on the beam pipe (BP)

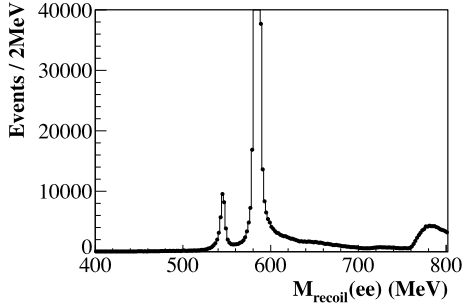


**Fig. 1.** Recoiling mass against the  $e^+e^-$  pair for the data sample after preselection cuts. The  $\phi \rightarrow \eta e^+e^-$  signal is clearly visible as the peak corresponding to the  $\eta$  mass.

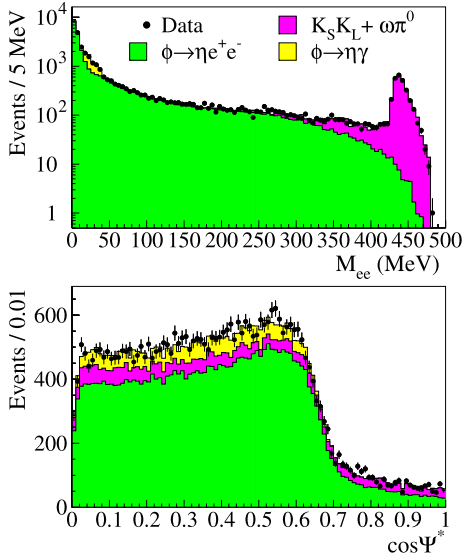


**Fig. 2.**  $\phi \rightarrow \eta e^+e^-$ ,  $\eta \rightarrow \pi^0 \pi^0 \pi^0$  events: data-MC comparison for  $M_{ee}$  (top) and  $\cos \Psi^*$  distributions (bottom) after the  $M_{\text{recoil}}(ee)$  cut. (For interpretation of the references to color in this figure legend, the reader is referred to the web version of this Letter.)

or drift chamber walls (DCW). After tracing back the tracks of the two  $e^+/e^-$  candidates, these events are efficiently rejected by reconstructing the invariant mass ( $M_{ee}$ ) and the distance ( $D_{ee}$ ) of the track pair both at the BP and DCW surfaces. Both variables are expected to be small for photon conversion events, so that this background is removed by rejecting events with:  $[M_{ee}(BP) < 10 \text{ MeV and } D_{ee}(BP) < 2 \text{ cm}]$  or  $[M_{ee}(DCW) < 120 \text{ MeV and } D_{ee}(DCW) < 4 \text{ cm}]$ .

At this stage of the analysis, the surviving background is dominated by events with two charged pions in the final state, and it is rejected by exploiting the timing capabilities of the calorimeter. When an energy cluster is associated to a track, the time of flight (ToF) to the calorimeter is evaluated both using the track trajectory ( $T_{\text{track}} = L_{\text{track}}/\beta c$ ) and the calorimeter timing ( $T_{\text{cluster}}$ ). The  $\Delta T = T_{\text{track}} - T_{\text{cluster}}$  variable is then evaluated in the electron hypothesis ( $\Delta T_e$ ). In order to be fully efficient on signal, events with either an  $e^+$  or an  $e^-$  candidate inside a  $3\sigma$  window around  $\Delta T_e = 0$  are retained for further analysis.

At the end of the analysis chain, 30577 events are selected, with  $\sim 3\%$  background contamination (Fig. 3). The analysis efficiency, defined as the ratio between events surviving analysis cuts and generated events, is  $\sim 15\%$  at low  $e^+e^-$  invariant masses, increasing up to 30% at higher  $M_{ee}$  values.

The analysis of the decay channel  $\eta \rightarrow \pi^+\pi^-\pi^0$  is the same as described in [10], with the addition of a cut on the recoil mass to

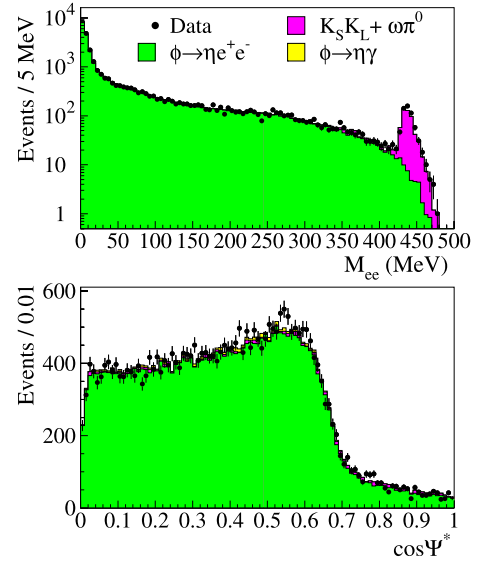


**Fig. 3.**  $\phi \rightarrow \eta e^+e^-$ ,  $\eta \rightarrow \pi^0 \pi^0 \pi^0$  events: data-MC comparison for  $M_{ee}$  (top) and  $\cos \Psi^*$  distributions (bottom) at the end of the analysis chain. (For interpretation of the references to color in this figure legend, the reader is referred to the web version of this Letter.)

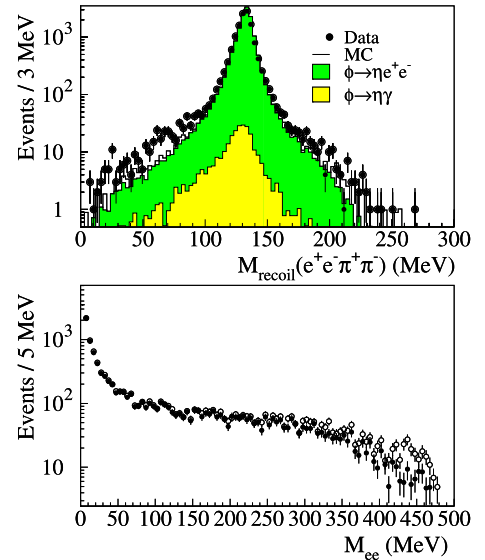


**Fig. 4.**  $\phi \rightarrow \eta e^+e^-$ ,  $\eta \rightarrow \pi^+\pi^-\pi^0$  analysis. Top: data-MC comparison for the recoil mass against the  $e^+e^-\pi^+\pi^-$  system. Bottom:  $M_{ee}$  distribution before (open circles) and after (black dots) the cut on  $M_{\text{recoil}}(ee\pi\pi)$ . (For interpretation of the references to color in this figure legend, the reader is referred to the web version of this Letter.)

the  $e^+e^-\pi^+\pi^-$  system, which is expected to be equal to the  $\pi^0$  mass for signal events. In Fig. 4 top, data-MC comparison shows some residual background contamination in the tails of the distribution, which are not well described by our simulation. A cut  $100 < M_{\text{recoil}}(ee\pi\pi) < 160 \text{ MeV}$  is then applied. The effect of this cut on the  $M_{ee}$  variable is shown in Fig. 4 bottom. The total number of selected events is 13254, with  $\sim 2\%$  background contamination.

#### 4. Upper limit evaluation on $U$ boson production

The upper limit on the  $U$  boson production in the  $\phi \rightarrow \eta U$  process is obtained combining the two  $\eta$  decay channels. The resolution of the  $e^+e^-$  invariant mass has been evaluated with a Gaussian fit to the difference between the reconstructed and

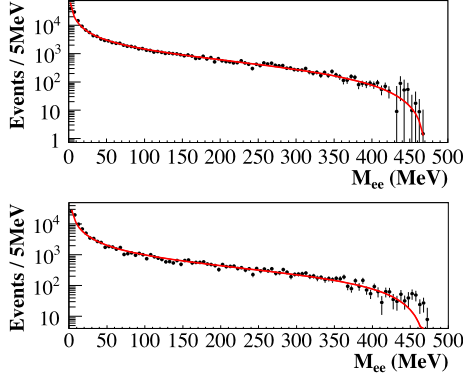


**Fig. 5.** Fit to the corrected  $M_{ee}$  spectrum for the Dalitz decays  $\phi \rightarrow \eta e^+ e^-$ , with  $\eta \rightarrow \pi^0 \pi^0 \pi^0$  (top) and  $\eta \rightarrow \pi^+ \pi^- \pi^0$  (bottom).

generated mass for Monte Carlo events, providing  $\sigma_{M_{ee}} \leq 2$  MeV over the whole  $M_{ee}$  range. The determination of the limit is done by varying the  $M_U$  mass, with 1 MeV step, in the range between 5 and 470 MeV. Only five bins (5 MeV width) of the reconstructed  $M_{ee}$  variable, centered at  $M_U$  are considered. For each channel, the irreducible background,  $b(M_U)$ , is extracted directly from our data after applying a bin-by-bin subtraction of the non-irreducible backgrounds and correcting for the analysis efficiency. The  $M_{ee}$  distribution is then fit, excluding the bins used for the upper limit evaluation. The parametrization of the fitting function has been taken from Ref. [15]. The  $\phi\eta\gamma^*$  transition form factor is parametrized as

$$F_{\phi\eta}(q^2) = \frac{1}{1 - q^2/\Lambda^2} \quad (1)$$

with  $q = M_{ee}$ . Free parameters are  $\Lambda$  and a normalization factor. The spread of the extracted parameters is contained within the statistical error of the fit done on the whole  $M_{ee}$  mass range, shown in Fig. 5, as expected from the overall good description of the  $M_{ee}$  shape for both  $\eta$  decay channels.

The exclusion limit on the number of events for the  $\phi \rightarrow \eta U$  signal as a function of  $M_U$  is obtained with the  $CL_S$  technique [16], using the  $M_{ee}$  spectra before background subtraction. The limit is extracted both for each  $\eta$  decay channel and in a combined way. For the combined procedure, the  $CL_S$  evaluation is done by summing values over all bins of the two decay channels, taking into account the different luminosity, efficiency and relative branching ratios of the two samples. The systematic error on the background knowledge  $\Delta b(M_{ee})$  is evaluated, for each  $M_U$  value, changing by one standard deviation the two fit parameters and has been taken into account while evaluating  $CL_S$ , applying a Gaussian spread of width  $\Delta b(M_{ee})$  on the background distribution. In Fig. 6 top, the upper limit at 90% C.L. on the number of events for the decay chain  $\phi \rightarrow \eta U$ ,  $U \rightarrow e^+ e^-$ , is shown for both  $\eta \rightarrow \pi^0 \pi^0 \pi^0$  and  $\eta \rightarrow \pi^+ \pi^- \pi^0$ , separately evaluated. In Fig. 6 bottom, the smoothed upper limit on the branching fraction for the process  $\phi \rightarrow \eta U$ ,  $U \rightarrow e^+ e^-$ , obtained from the combined method is compared with evaluations from each of the two decay channels. In the combined result, the upper limit on the product  $BR(\phi \rightarrow \eta U) \times BR(U \rightarrow e^+ e^-)$  varies from  $10^{-6}$  at small  $M_U$  to  $\sim 3 \times 10^{-8}$  at 450 MeV.

The exclusion plot in the  $\alpha'/\alpha = \epsilon^2$  vs  $M_U$  plane, where  $\alpha'$  is the coupling of the  $U$  boson to electrons and  $\alpha$  is the fine structure constant, has been finally derived assuming the relation [9]:

$$\sigma(e^+ e^- \text{ to } \phi \rightarrow \eta U) = \epsilon^2 |F_{\phi\eta}(m_U^2)|^2 \frac{\lambda^{3/2}(m_\phi^2, m_\eta^2, m_U^2)}{\lambda^{3/2}(m_\phi^2, m_\eta^2, 0)} \sigma(e^+ e^- \rightarrow \phi \rightarrow \eta\gamma), \quad (2)$$

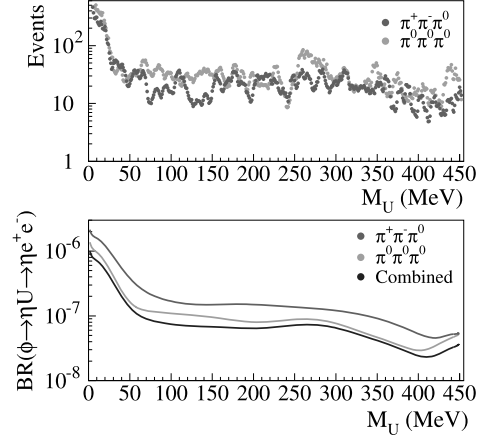


**Fig. 6.** Top: upper limit at 90% C.L. on the number of events for the decay chain  $\phi \rightarrow \eta U$ ,  $U \rightarrow e^+ e^-$ , with  $\eta \rightarrow \pi^0 \pi^0 \pi^0$  and  $\eta \rightarrow \pi^+ \pi^- \pi^0$ . Bottom: smoothed upper limit at 90% C.L. on  $BR(\phi \rightarrow \eta U) \times BR(U \rightarrow e^+ e^-)$ , obtained separately for the two  $\eta$  decay channels and from the combined analysis.

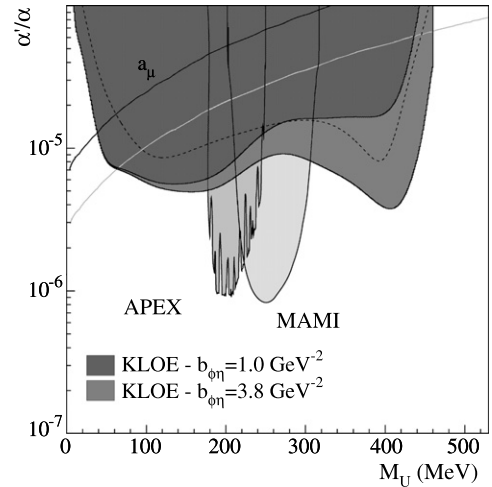


**Fig. 7.** Exclusion plot at 90% C.L. for the parameter  $\alpha'/\alpha = \epsilon^2$ , compared with existing limits from the muon anomalous magnetic moment and from MAMI/A1 and APEX experiments. The gray line represents the expected values of the  $U$  boson parameters needed to explain the observed discrepancy between measured and calculated  $a_\mu$  values. The dotted line is the previous KLOE result, obtained with the  $\eta \rightarrow \pi^+ \pi^- \pi^0$  channel only.

with  $\lambda(m_1^2, m_2^2, m_3^2) = [1 + m_3^2/(m_1^2 - m_2^2)]^2 - 4m_1^2 m_3^2/(m_1^2 - m_2^2)^2$ . We assume that the  $U$  boson decays only to lepton pairs, with equal coupling to  $e^+ e^-$  and  $\mu^+ \mu^-$ .

The extraction of the limit on the  $\alpha'/\alpha$  parameter is related to the parametrization of the form factor (Eq. (2)), and thus to the  $\Lambda$  parameter in Eq. (1). The SND experiment measured the form factor slope,  $b_{\phi\eta} = dF/dq^2|_{q^2=0} = \Lambda^{-2}$ , obtaining  $b_{\phi\eta} = (3.8 \pm 1.8) \text{ GeV}^{-2}$  [17], with a central value different from theoretical predictions based on VMD ( $b_{\phi\eta} \sim 1 \text{ GeV}^{-2}$ ) [18], although in agreement within the error. In Fig. 7 the smoothed exclusion plot at 90% C.L. on  $\alpha'/\alpha$  is compared with existing limits in the same region of interest [6,7,19]. The evaluation is done using both the experimental and the theoretical values of the form factor slope. The two resulting curves overlap at low  $M_{ee}$  values, while the limit obtained using the SND measurement gives an increasingly larger exclusion region up to  $\sim 400$  MeV, moving closer to the other curve at the end of the phase space. Having the experimental value of  $b_{\phi\eta}$  an uncertainty of  $\sim 50\%$ , we conservatively use the curve obtained with theoretical predictions, resulting in

a limit of:  $\alpha'/\alpha < 1.7 \times 10^{-5}$  for  $30 < M_U < 400$  MeV, and even better for the sub-region  $50 < M_U < 210$  MeV:  $\alpha'/\alpha < 8.0 \times 10^{-6}$ . Comparing our result with the previous KLOE measurement, reported as the dotted line in Fig. 7, we improve the upper limit of about a factor of two when using the same parametrization of the form factor. This result reduces the region of the  $U$  boson parameters that could explain the observed discrepancy between the measurement and Standard Model prediction of the muon anomalous magnetic moment,  $a_\mu$ , ruling out masses in the range 60–435 MeV.

### Acknowledgements

We warmly thank our former KLOE colleagues for the access to the data collected during the KLOE data taking campaign. We thank the DAΦNE team for their efforts in maintaining low background running conditions and their collaboration during all data taking. We want to thank our technical staff: G.F. Fortugno and F. Sborzacchi for their dedication in ensuring efficient operation of the KLOE computing facilities; M. Anelli for his continuous attention to the gas system and detector safety; A. Balla, M. Gatta, G. Corradi and G. Papalino for electronics maintenance; M. Santoni, G. Paoluzzi and R. Rosellini for general detector support; C. Piscitelli for his help during major maintenance periods. This work was supported in part by the EU Integrated Infrastructure Initiative Hadron Physics Project under contract number RII3-CT-2004-506078; by the European

Commission under the 7th Framework Programme through the ‘Research Infrastructures’ action of the ‘Capacities’ Programme, Call: FP7-INFRASTRUCTURES-2008-1, Grant Agreement No. 227431; by the Polish National Science Centre through the Grants No. 0469/B/H03/2009/37, 0309/B/H03/2011/40, DEC-2011/03/N/ST2/02641, 2011/01/D/ST2/00748 and by the Foundation for Polish Science through the MPD programme and the project HOMING PLUS BIS/2011-4/3.

### References

- [1] P. Fayet, Phys. Lett. B 95 (1980) 285.
- [2] B. Batell, M. Pospelov, A. Ritz, Phys. Rev. D 80 (2009) 095024.
- [3] N. Arkani-Hamed, N. Weiner, JHEP 0812 (2008) 104.
- [4] M. Pospelov, A. Ritz, M.B. Voloshin, Phys. Lett. B 662 (2008) 53.
- [5] B. Holdom, Phys. Lett. B 166 (1986) 196.
- [6] H. Merkel, et al., Phys. Rev. Lett. 106 (2011) 251802.
- [7] S. Abrahamyan, et al., Phys. Rev. Lett. 107 (2011) 191804.
- [8] J.P. Lees, et al., Phys. Rev. Lett. 108 (2012) 211801.
- [9] M. Reece, L.T. Wang, JHEP 0907 (2009) 051.
- [10] F. Archilli, et al., Phys. Lett. B 706 (2012) 251.
- [11] M. Adinolfi, et al., Nucl. Instr. Meth. A 488 (2002) 51.
- [12] M. Adinolfi, et al., Nucl. Instr. Meth. A 482 (2002) 364.
- [13] M. Adinolfi, et al., Nucl. Instr. Meth. A 492 (2002) 134.
- [14] F. Ambrosino, et al., Nucl. Instr. Meth. A 534 (2004) 403.
- [15] L.G. Landsberg, Phys. Rep. 128 (1985) 301.
- [16] T. Junk, Nucl. Instr. Meth. A 434 (1999) 435.
- [17] M.N. Achasov, et al., Phys. Lett. B 504 (2001) 275.
- [18] N.N. Achasov, A.A. Kozhevnikov, Sov. J. Nucl. Phys. 55 (1992) 449.
- [19] M. Pospelov, Phys. Rev. D 80 (2009) 095002.